UC Merced

UC Merced Previously Published Works

Title

Arene Substitution Design for Controlled Conformational Changes of Dibenzocycloocta-1,5-dienes

Permalink

https://escholarship.org/uc/item/18w3449x

Journal

Journal of the American Chemical Society, 142(39)

Authors

Fu, Wenxin
Alam, Todd M
Li, Jiachen
et al.

Supplemental Material

https://escholarship.org/uc/item/18w3449x#supplemental

Peer reviewed

Arene Substitution Design for Controlled Conformational Changes of Dibenzocycloocta-1,5-dienes

Wenxin Fu,[1] Todd M. Alam,[2] Jiachen Li,[3] Jacqueline Bustamante,[1] Thanh Lien,[4] Ralph W. Adams,[5] Simon J. Teat,[6] Benjamin J. Stokes,[4] Weitao Yang,[3] Yi Liu,[7] Jennifer Q. Lu[1,*]

[1]Materials Science and Engineering, School of Engineering, University of California, Merced, 5200 North Lake Road, Merced, California 95343, USA. *Email: jlu5@ucmerced.edu

[2]Department of Organic Material Sciences, Sandia National Laboratories, Albuquerque, NM 87185

[3]Department of Chemistry and Department of Physics, Duke University, Durham, North Carolina 27708, USA

[4]Department of Chemistry and Chemical Biology, University of California, Merced, 5200 North Lake Road, Merced, California 95343, USA

[5]Department of Chemistry, The University of Manchester, Oxford Road, Manchester, M13 9PL, United Kingdom

[6]Advanced Light Source, Lawrence Berkeley National Laboratory, Berkeley, California 94720, United States

[7]The Molecular Foundry, Lawrence Berkeley National Laboratory, One Cyclotron Road, Berkeley, California 94720, United States

ABSTRACT: We report that the agile eight-membered cycloalkane can be stabilized by fusing two rigid benzene rings, substituted with proper functional groups. The conformational change of dibenzocycloocta-1,5-diene (DBCOD), a rigid-flexible-rigid organic moiety, from Boat to Chair conformation requires an activation energy of 42 kJ/mol that is substantially lower than that of existing submolecular shape-changing unit. Experimental data corroborated by theory calculations demonstrate that intramolecular hydrogen bonding can stabilize Boat whereas electron repulsive interaction from opposing ester substituents favors Chair. Intramolecular hydrogen bonding, formed by 1,10-diamide substitution stabilizes Boat, spiking the temperature at which Boat and Chair can readily interchange from –60 °C to 60 °C. Concomitantly this intramolecular attraction raises the energy barrier from 42 kJ/mol of unsubstituted DBCOD to 68 kJ/mol of diamide-substituted DBCOD. Remarkably, this value falls within the range of the activation energy of highly efficient enzyme catalyzed biological reactions. With shape changes once considered only possible with high-energy, our work reveals a potential pathway exemplified by a specific submolecular structure to achieve low-energy driven shape changes for the first time. Together with intrinsic cycle stability and high energy output systems that would have incurred damage under high-energy stimuli, could particularly benefit from this new kind of low-energy driven shape-changing mechanism. This work has laid the basis to construct systems for low-energy driven stimuli-responsive applications, hitherto a challenge to overcome.

INTRODUCTION

Molecular- and submolecular-level shape changes in response to an external stimulus serves as a foundation to enable low-energy driven actuations, such as biomanipulators (*e.g.*, tweezers and gear,[1] and ion channel regulation[2]), controlled drug release,[3] regenerative medicine (*e.g.*, dynamic scaffolds,[4] and artificial muscle[5]), adaptive architectural systems (*e.g.*, "heliophilic" optics[6]), soft robotics,[7-8] deployable structures (such as erectable trusses and inflatable solar concentrators),[9-11] and memory and logic devices.[12-13] Typically stimulus is based on chemical (phenanthroline/copper redox combination,[14] hydrazine,[15-16] and biphenyl motor[17]), or electrochemical reaction (thiophenylidene derivative[18] and π-donor/π-acceptor systems[19]), as well as photoinduced isomerization (azobenzene,[20] stilbene-containing,[21] dicyanoethene[22] and hydrazone[23]) or cyclization (diarylethene,[24-25] spiropyran,[26] and fulgide[27-28]). The major limitation of chemically or electrochemically activated systems is medium

dependence. Photon stimulus offers advantages, such as high speed and spatiotemporal resolution using remote optical stimuli.[29] However, conventional photon-enabled submolecular shape-changing structures intrinsically require a high-energy stimulus, *i.e.,* ultraviolet light for the conversion from the ground state to an excited state. These high-energy stimuli are responsible for photobleaching and harmful to biological species. Several decades of research have developed molecular structures that respond to longer irradiation wavelengths including visible and infrared light.[30-34] However, limitations include strong medium dependence, spontaneous reversal, and inadequate cycle stability. Intrinsically, molecules below one micron from a surface can't be stimulated due to limited penetration of light stimulus.[35] This limits the maximum energy output. Numerous real-world applications require new types of submolecular shape-changing structures that can be addressed by low-energy stimuli.

Nature provides an endless repertoire of low-energy driven conformational changes in response to chemical stimuli to drive conformation in order to readily bind carbon dioxide for disposal.[36] The conformational change of a G protein-coupled receptor (GPCR) activates a nearby G protein, leading to the production of secondary messengers. Through a sequence of events, GPCRs regulate an incredible range of bodily functions, from sensation to hormone responses.[37] Displaying power-efficiency, reliability and reproducibility, these molecular-level conformational transitions serve as an inspirational model and control diverse cellular processes. For instance, hemoglobin delivers oxygen throughout the body, and then changes its .

Dibenzocycloocta-1,5-diene, DBCOD, features a flexible central eight-membered cycloalkane with rigid phenyl rings fused onto each end (Scheme 1a). We have revealed DBCOD-containing polymers exhibiting significant thermal contraction[38-40] despite containing only a small amount of tetraphenylamide substituted DBCOD. Theoretical calculations implied that this substantial thermal contraction might be the result of the DBCOD conformational change from Boat (global minimum) to Chair conformation (local minimum) upon heating (Scheme 1b).[39]

To examine this hypothesis, we have synthesized a library of DBCODs bearing various substituents (Scheme 2). Through variable temperature NMR (VT-NMR) spectroscopic characterization and density functional theory (DFT) investigation, we discovered that intramolecular interactions can substantially regulate DBCOD conformational dynamics. *Trans* to *cis* isomerization of azobenzene requires an activation energy of at least 150 kJ/mol and very often in excess of 250 kJ/mol.[41-42] In stark contrast, 2,3,8,9-tetramethyl substituted DBCOD

(TM-DBCOD) requires 3 times less energy, approximately 40 kJ/mol, which is similar to the reported value of unsubstituted DBCOD.[43] Aldehyde-functionalized TM-DBCOD on carbons at 1 and 10 positions can raise the activation energy ($\Delta G^{\ddagger}$) to 55 kJ/mol. Boat stabilization stems from two hydrogen bonds between the oxygen from a water molecule and the two hydrogens located on the aldehyde groups. On the other hand, for 2,9-dialdehyde substituted DBCOD, two CHO groups sit too far from each other to form a water bridge via two hydrogen bonds, thus requiring only 44 kJ/mol for the Boat to Chair conversion.

The strong intramolecular hydrogen bond imposed by 1,10-diamide substituents resulted in an activation energy of about 68 kJ/mol, equivalent to the photon energy of near infrared light of 1500 to 1600 nm.[44] The value falls within the range of activation energy of 50 – 80 kJ/mol of enzyme catalyzed biological reactions, such as decarboxylation by orotidine-5′-monophosphate decarboxylase,[45] methyl transfer reaction by catechol *O*-methyltransferase[46] and oxidative deamination by D-amino acid oxidase.[47]

Comparing 1, 10 diethyl ester with 1,10 diethyl amide, intramolecular hydrogen bonding favors Boat while electron repulsive force yields more Chair. Indeed, at room temperature, 1,10-di-Et-ester revealed 86 % Chair whereas 14 % Chair was found in 1,10-di-Et-amide. The temperature at which Boat and Chair can be interchanged readily for 1, 10 diethyl ester is -35 ∘C whereas 50 ∘C for 1,10 diethyl amide.

Our study demonstrates, for the first time, that judicious molecular design and tailored substitution open a way for harnessing low-energy conformational changes of medium-sized hydrocarbon rings. The molecular chassis and substituent design principles described herein could herald a new category of submolecular shape-changing structures that do not require high-energy stimuli, unlike conventional ones. This new low-energy driven mechanism pushes the application frontier -- introducing this unit into molecular-, nano- and macro-scale systems, allows low energy stimuli such as near infrared and magnetic induced local temperature elevations, to regulate systems' property or function. For example, incorporating this structure into liquid crystal, actuation/switch can occur using low-energy sources. Due to the high penetration depth of low-energy stimuli, we expect that actuation based on this conformational change mechanism possesses significantly higher energy density than conventional systems.

RESULTS AND DISCUSSION

Synthesis of Functional Group Substituted DBCOD Derivatives. TM-DBCOD and its 1,10-disubstituted derivatives, including dialdehyde (1,10-di-CHO), diphenylester (1,10-di-Ph-ester), diethylester (1,10-di-Et-ester), diphenylamide

(1,10-di-Ph-amide) and diethylamide (1,10-di-Et-amide) substituted TM-DBCOD, were synthesized according to the synthetic route shown in Scheme 2. 2,9-dialdehyde substituted DBCOD (2,9-di-CHO) was prepared based on our previous published paper[48] and used as a control to study the effect of substitution positions on the DBCOD conformational dynamics.

Specifically, TM-DBCOD was synthesized from (4,5-dimethyl-1,2-phenylene)dimethanol (di-OH) on a large scale, sequentially through bromination[49] using phosphorous tribromide and dimerization[50-51] in the presence of lithium sands. 1,10-di-CHO was formed *via* Rieche formylation.[52-53] One-step column purification of 1,10-di-CHO was adequate instead of multi-step column purification required for the preparation of 2,9-di-CHO (Scheme S1 and Figure S1-2).[54] Because there are only four possible positions for the formylation of TM-DBCOD, fewer than those of 1,2:5,6-dibenzocyclooctadiene (DBCOD). Therefore, the 1,10-di-CHO can be easily distinguished and separated from its 1,7-diformylated isomer by flash column purification.[52] Finally, 1,10-di-Et-ester, 1,10-di-Ph-ester, 1,10-di-Et-amide and 1,10-di-Ph-amide were successfully prepared through oxidation with hydrogen peroxide and sodium chlorite,[55] followed by acyl chlorination using thionyl chloride and esterification/amidation using respective alcohol or amine. The chemical structures of this series of DBCOD derivatives were confirmed by ^{1}H and ^{13}C NMR spectroscopy (Figure S3-S18).

Variable Temperature ^{1}H-NMR Studies of DBCOD Conformational Dynamics. Variable temperature ^{1}H-NMR spectroscopy (VT ^{1}H-NMR) has been used to study the conformational changes of medium-sized rings.[56-57] Through the analysis of VT ^{1}H-NMR, activation energy ($\Delta G^{\ddagger}$) corresponding to the energy difference between the global minimum and transition state, as well as the Gibbs free energy (ΔG^{o}) between Boat and Chair can be obtained. The coalescence temperature (T_c) is defined as the temperature at which the rate of exchange between Boat and Chair approaches to the NMR experiment time scale. Below T_c, the distinct peaks from Boat and Chair conformations show up and their respective populations can be calculated based on the ratio of integrations. At and above T_c, a single broadened signal, observed due to fast exchange, is a result of the population-weighted average of two conformers. Therefore, we can use the distance between the observed chemical shift at each given temperature above T_c in relation to the individual Boat or Chair position to estimate Boat and Chair population as a function of temperature. VT ^{1}H-NMR analyses were conducted using low polarity CD_2Cl_2 and non-polar CS_2 with the volume ratio of 4/1 for TM-DBCOD, 1,10-di-CHO, 2,9-di-CHO and 1,10-diesters. High polarity solvent DMSO-d_6 was adopted for 1,10-diamides. A series of mixtures of DMSO-d_6 and CD_2Cl_2 at different ratios was used to understand the effect of solvent polarity on the conformational properties of 1,10-di-Ph-amide.

Density functional theory (DFT) predicted ^{1}H-NMR chemical shifts for the Boat and Chair conformers of TM-DBCOD and its derivatives were summarized in Table S1. The calculated chemical shifts were used to aid the assignment of proton signals in either Boat or Chair conformation (Figure 1-3). Molecular symmetry differences caused by substitution along with different spatial arrangements for Boat and Chair conformations afford multiple inequivalent methylene and methyl protons. Experimentally, with increasing temperature the ring dynamics simplified the ^{1}H-NMR spectra, reducing the number of signals through the averaging of multiple chemical shifts.

(i) 2,3,8,9-tetramethyl substituted DBCOD (TM-DBCOD)

Taking TM-DBCOD at – 80 °C as an example (Figure 1a), the aromatic protons gave two signals (δ = 6.95 and 6.69) and the methylene protons gave one broad signal along with two doublets (δ = 3.05 and δ = 2.96, 2.47). Previous reports[58-59] stated that two nonequivalent methylene protons in the Chair conformer should generate an AB quartet (four lines), whereas the Boat conformer should exhibit two AB quartet patterns (eight lines). If the temperature was sufficiently low to slow down the conversion of Boat conformers, two quartet peaks should appear. Even at – 80 °C, the broaden methylene resonances for Boat configuration were not well resolved, demonstrating rapid conformational averaging existed at this low temperature. The high-intensity and broad peak (δ = 3.05) was assigned to the Boat conformer[59] whereas two doublets (δ = 2.96 and 2.47) were assigned to the Chair conformer. DFT calculated ^{1}H chemical shifts (Table S1) indicated that methylene (-CH_2-) chemical shifts between 2.9 and 2.6 ppm belonged to Chair, whereas chemical shifts occurring between 3.43 and 2.77 ppm were assigned to Boat.

Using the integrals of two sets of methyl protons, relative populations of Chair and Boat can be calculated as 13 % and 87 %, respectively. At – 60 °C, the NMR resonances, including both aromatic protons (δ = 6.77) and methylene protons on the eight-membered ring (δ = 3.04), appeared as broadened singlets due to intermediate exchange. It can be assumed that the population of Chair and Boat influenced the observed NMR chemical shift. The fact that the NMR resonance belonging to aromatic proton moved towards the predicted chemical shift of Chair was indicative of rising Chair population with increasing temperature.

(ii) 1,10- and 2,9-dialdehyde substituted DBCOD derivatives

For 1,10-di-CHO at low temperatures (– 80 and – 60 °C) (Figure 1b), both the deshielded aldehyde and aromatic protons split into two singlets (δ = 10.66, 10.47, and δ = 7.24, 6.92). The tetramethyl protons gave two sets of two singlets (δ = 2.40, 2.30, and δ = 2.21, 2.15), while the methylene protons appeared as a series of multiplets. The more intense set (δ = 3.49, 3.39, 3.10, 2.90) corresponded to the different chemical environments of -CH_2- on the eight-member ring in the Boat conformer as predicted by DFT calculations (Table S1). Another downfield-shifted minor set of resonances observed at – 80 °C was the tiny singlet from aldehyde proton (δ = 10.66) and aromatic proton (δ = 7.24), together with the doublets from methylene protons (δ = 3.54 and 2.64), indicating the presence of a small portion of Chair. The relative populations of Boat and Chair can be calculated using methyl proton, yielding 94 % Boat and 6 % Chair at – 80 °C. Comparing with 87 % Boat and 13 % Chair for TM-DBCOD at the same temperature, we concluded that 1,10-dialdehyde substitution stabilized the Boat conformation. This was corroborated by the coalescence temperature (T_c) of – 35 °C for 1,10-di-CHO, as opposed to – 60 °C for TM-DBCOD.

We also studied the VT ^{1}H-NMR spectra of 2,9-dialdehyde substituted DBCOD (2,9-di-CHO) (Figure 1c) with each aldehyde functional group one atomic position away from the eight-membered ring in contrast to 1,10-di-CHO. The calculated relative populations of Boat and Chair for 2,9-di-CHO at – 80 °C were 91 % and 9 %, using the aldehyde proton signals (δ = 9.76 for Boat and δ = 9.96 for Chair). The observed T_c for 2,9-di-CHO was similar to that for the unsubstituted TM-DBCOD.

DFT calculations of 1,10-di-CHO molecule indicated (Figure S19a) that a water molecule can form hydrogen bonds with the aldehyde group at 1 and 10 positions respectively and thus stabilizing Boat conformation. This was verified by differential scanning calorimetry (DSC) (Figure S20). An endothermic peak at around – 30 °C was observed during the first two runs but disappeared after repeated heating cycles under dry N_2 without taking the pan out. After leaving the pierced DSC pan exposed to air for an extended period time, the endothermic peak reappeared, suggesting that this is water-related. Therefore, this endothermic peak at around – 30 °C was a result of the release of water molecules. According to VT-^{1}H NMR spectra of 1,10-di-CHO (Figure S21), water is present.

On the contrary, the 2,9-di-CHO did not produce a detectable DSC peak. This is due to the greater geographic separation between two aldehydes preventing water from bridging two aldehydes via hydrogen bonding interaction, predicted by DFT (Figure S19b).

(iii) 1,10-diamide substituted TM-DBCODs

Figure 2a is VT ^{1}H-NMR spectra of 1,10-di-Et-amide. According to DFT predictions (Table S1), the chemical shifts of both methyl and aromatic protons in Chair should be more downfield shifted than those of Boat. One could rationally deduce that the minor peak of aromatic proton (δ = 6.95) belonged to Chair and the major one (δ = 6.77) corresponded to Boat. Similar results can be found for the methyl protons (δ = 2.15 for Chair and δ = 2.06, 1.94 for Boat). Based on integration of methyl peaks, relative populations were 14 % Chair and 86 % Boat at 23 °C. T_c was about 50 °C. The result reinforced the postulation that intramolecular hydrogen bonding could raise the activation energy for the dynamic conversion.

The VT ^{1}H-NMR spectra of 1,10-di-Ph-amide also displayed both sets of peaks associated with aromatic and methyl protons (Figure 2b). Similarly, we assigned the smaller peaks of methyl protons (δ = 2.20 and 2.12) as Chair, and the more significant ones (δ = 2.15 and 2.06) as Boat. Peak integration of methyl protons yielded the relative population of Chair and Boat as 28 % and 72 %, respectively, at 23 °C. The reason that the Chair population of 1,10-di-Ph-amide of 28 % at 23 °C was twice as that of 1,10-di-Et-amide of 14 % at the same temperature was most likely caused by the steric hindrance effect imposed by phenyl rings on 1,10 substitutions of DBCOD to retard the formation of Boat. Meanwhile, T_c was observed at 60 °C.

The chemical shift changes of methylene protons with increasing temperatures (Figure 2c) also confirmed that the coalescence of two conformations for both diamide substituted DBCODs in DMSO occurred above room temperature. The averaged two singlets of methylene proton at 90 °C for 1,10-di-Ph-amide (δ = 2.96, 3.0) and for 1,10-di-Et-amide (δ = 2.97, 2.88) changed into two broadened resonances with shoulder peaks at 40 °C and below,

Table 1. Relative molar ratio of Boat/Chair for different DBCOD derivatives at different temperatures and the corresponding T_c

Compound	Relative molar ratio of Boat/Chair at different T	Coalescence Temperature (T_c) (°C)
TM-DBCOD	87/13[a]	-60
1,10-di-CHO	94/6[a] 90/10[b]	-35
2,9-di-CHO	91/9[a]	-60
1,10-di-Et-ester	59/41[b]	-35
1,10-di-Ph-ester	66/34[b]	-35
1,10-di-Et-amide	86/14[c]	50
1,10-di-Ph-amide	72/28[c]	60

[a]: -80 °C. [b]: -60 °C. [c]: 23 °C.

indicating the slow exchange of Boat and Chair conformation.

It is known that solvent polarity impacts the energy barrier of isomerization.[60-62] To examine this effect, we performed ^{1}H-NMR studies using different volume ratios of high polarity solvent DMSO-d$_6$ and the low polarity solvent CD$_2$Cl$_2$ (Figure 2d). The Boat population increased with a higher percentage of CD$_2$Cl$_2$ in the solvent mixture, i.e., reducing polarity. This result implied that DMSO can effectively break the DBCOD intramolecular hydrogen bond and destabilize Boat.

(iv) 1,10-diester substituted TM-DBCODs

The VT ^{1}H-NMR results of 1,10-di-Et-ester and 1,10-di-Ph-ester at – 60 °C clearly indicated the presence of two conformers (Figure 3a and 3b). DFT calculations (Table S1) also indicated that both the chemical shifts of aromatic and methyl protons produced by Chair should be more downfield than those produced by Boat.

Moreover, for 1,10-di-Et-ester, four sets of methylene doublets (δ = 2.38, 2.55, 2.77 and 3.02) were assigned to Chair, while two broad peaks (δ = 2.98 and 3.10) belonged to Boat. Analogously, the assignments of Chair and Boat for 1,10-di-Ph-ester can be found in Figure 3b. Based on the integrals of two sets of methyl protons on DBCOD, relative populations were 41 % Chair and 59 % Boat for 1,10-di-Et-ester and 34 % Chair and 66 % Boat for 1,10-di-Ph-ester at – 60 °C.

The remarkable difference of Boat and Chair populations between 1,10-dialdehyde and 1,10-diester substituted DBCODs at – 60 °C was originated from their distinct intramolecular interactions. In comparison with 1,10-di-Et-ester, π-π stacking interaction of two appended phenyl rings as parts of two opposing phenyl ester groups can be spatially arranged to stabilize Boat (Figure 3c). At – 60 °C, the 1,10-di-Ph-ester therefore yielded a higher Boat population, 66 %, as opposed to 59 % of 1,10-di-Et-ester. Due to hydrogen bonds formed between an encased water molecule and 1,10-dialdehyde groups, 90 % Boat was present in 1,10-di-CHO at – 60 °C. The electrostatic repulsive interaction between two adjacent ester groups of 1,10-diesters destabilized Boat, resulting in a 2 – 3 times higher Chair population for 1,10-diesters than that for 1,10-di-CHO at – 60 °C.

Displacing ethyl groups with phenyl groups mitigated repulsive interaction and together with the additional π-π interaction generated by two adjacent phenyl rings shifted the equilibrium towards Boat. Table 1 demonstrated preferred conformations and coalescence temperatures of DBCOD derivatives. Boat population and activation energy increased with introducing intramolecular hydrogen bond. The electric repulsive interaction favored Chair. Therefore, the

DCBOD conformational dynamics can be modulated by substitution.

Since the conformational changes of DBCOD derivatives between Boat and Chair doesn't involve any covalent bond disruption/formation, it is intrinsically reversible. This contention is exemplified by the VT-^{1}H NMR analysis of 1,10-di-Ph-amide in DMSO-d$_6$ upon heating and cooling (Figure S22).

Kinetic and Thermodynamic Study of DBCOD Conformational Conversion

(i) Theoretical and experimental investigation of conformational kinetics

The VT ^{1}H-NMR analysis yielded DBCOD conformational exchange rates, entropy of activation ($\Delta S^{\ddagger}$), and enthalpy of activation ($\Delta H^{\ddagger}$) (Table S2). We observed negative values of entropy of activation which varied significantly. Increasing intramolecular forces formed by the neighboring substituents produced greater negative $\Delta S^{\ddagger}$ values. These values implied that intramolecular interactions reduce the degrees of molecular freedom leading to a higher entropic penalty for a conformational change. This result demonstrated that the conformation kinetics can be readily tailored through entropy of activation which itself can be modulated by substitution (Figure 4a). Related studies of azobenzene isomerization also revealed the negative entropy,[60, 62-64] more ordered activated complex during isomerization.

The activation energies ($\Delta G^{\ddagger}$) of DBCOD derivatives obtained from VT ^{1}H-NMR analysis and DFT calculations were compared side-by-side in Table S3. 2, 9 substitution inconsiderably impacted on activation energy. Because two aldehyde groups at 2, 9 positions were too far apart to interact with each other, 2,9-di-CHO had similar activation energy to that of TM-DBCOD. On the contrary, the two neighboring amide groups at the 1, 10 positions formed a strong intramolecular hydrogen bond (HNC=O···HNC=O), raising the activation energy to 68 kJ/mol, a 60 % increase over that of unsubstituted TM-DBCOD. The two weak hydrogen bonds between water and the 1,10-substituted aldehyde pair resulted in an activation energy of 55 kJ/mol for 1,10-di-CHO. Electron density map of 1,10-diester derivatives indicated that ester groups offered appreciable electrostatic repulsive interaction (Figure S23), rendering activation energies around 50 kJ/mol. DFT calculations closely matched with experimental results throughout (Figure 4a).

Furthermore, $\Delta H^{\ddagger}$ varied linearly with $\Delta S^{\ddagger}$ as a function of $\Delta H^{\ddagger}=45.68+0.11\Delta S^{\ddagger}$ (Figure S24). The DBCOD conformational change showed a typical enthalpy-entropy compensation effect.[65] This result indicated that substitution altered neither the conformational change pathway nor mechanism. Analogously to the *cis-trans* isomerization of azobenzene-based molecules with different substitutions, enthalpies of

activations are not sensitive to substitution properties.[63]

(ii) Theoretical and experimental investigation of conformational energetics

DFT study (Table S4) revealed that intramolecular forces significantly affected the conformation equilibrium position between Boat and Chair. Intramolecular interactions generated by hydrogen bonding and π-π stacking steered the equilibrium position towards Boat. This trend foreseen by computation agreed with experimental results (Figure 4b). Without intramolecular interactions, Chair conformers of TM-DBCOD were thermodynamically favored at 25 °C. Electrostatic repulsive interaction of 1,10-diester groups afforded more Chair than that of TM-DBCOD. This led to more negative values of Gibbs free energy (ΔG^o) of 1,10-diester substituted DBCODs compared with TM-DBCOD.

For 1,10-diamide substitution, the intramolecular hydrogen bond formed by two adjacent diamides rendered Boat as the global minimum at 25 °C. Preference of Boat over Chair yielded a positive value of ΔG^o at 25 °C. For example, DFT calculations predicted ΔG^o values of 6.4 and 2.6 kJ/mol at 25 °C for 1,10-di-Et-amide and 1,10-di-Ph-amide, respectively. Experimentally, we observed the similar trend, ΔG^o values are positive at 25 °C.

According to VT ^{1}H-NMR analysis, the populations of Boat and Chair for each DBCOD derivative at different temperatures were estimated as shown in Table S5 and Figure S25a-g. Indeed, at 23 °C, 1,10-di-Et-amide presented as 86 % Boat as opposed to 72 % Boat in 1,10-di-Ph-amide. In stark contrast, unsubstituted TM-DBCOD could sustain 87% Boat only at –80 °C. This over 100 °C difference further supported the contention that intramolecular hydrogen bonding can effectively stabilize Boat. 1,10-di-Ph-amide at 23 °C adopted 72 % of Boat but the Boat population dropped to 27 % at 90 °C. Comparing 1,10-di-Et-ester with 1,10-di-Et-amide, intramolecular hydrogen bonding favored Boat while electron repulsive force yielded more Chair. Indeed, at room temperature, 1,10-di-Et-ester had 86 % of Chair whereas 14 % of Chair was found in 1,10-di-Et-amide. The change of population with temperature forms the foundation of thermally driven shape-changing submolecular structures.

While theory calculations and experiment data revealed the same trend, the discrepancy in magnitude between theory and experimental results of diesters might be due to the fact that theory calculations do not consider the effect of solvent on electrostatic interaction.

Small-molecule X-ray Crystallography. DFT calculations of two units of TM-DBCOD and 1,10-di-Et-amide molecules respectively were used to study molecular packing configuration in crystal. Adding one more TM-DBCOD molecule favored

Chair, reducing ΔG^o from – 3.6 kJ/mol to – 7.9 kJ/mol (Table S4). Due to intermolecular π-π stacking formed between phenyl rings from neighboring TM-DBCOD, Chair became more favorable for TM-DBCOD which was absent of intramolecular interactions. The X-ray crystallography of TM-DBCOD (Figure 5a) confirmed the theoretical prediction, showing two stacked TM-DBCODs in the Chair conformation, agreeing well with prior published data of unsubstituted DBCOD.[66]

Based on DFT, the intramolecular hydrogen bonding was sufficiently large to favor Boat conformation. According to X-ray crystallography, 1,10-di-Et-amide adopted the Boat conformation, π-π stacking along the opposite sides of two Boats and oriented upside down relative to each other in crystal (Figure 5b). This finding highlights the importance of intra- and inter-molecular interactions on the DBCOD conformation state. In solid, the interplay of these two joint forces dictate the DBCOD conformation dynamics.
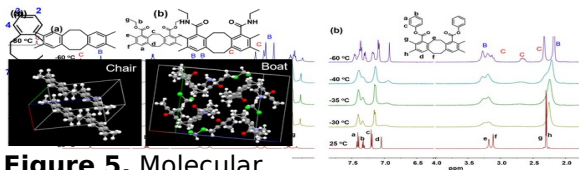
Figure 5. Molecular structure and spatial configuration based on small-molecule X-ray crystallography of (a) TM-DBCOD and (b) 1,10-di-Et-amide. Dark grey: Carbon; white: Hydrogen, menthe: Oxygen; purple: Nitrogen and green: Chlorine (solvent).

Figure 4. (a) Kinetic and (b) energetic Gibbs free energy changes of DBCOD derivatives at 25 °C, respectively, with one water molecule encased (left), 1,10-di-Ph-ester (middle) and 1,10-di-Et-ester (right). (black: carbon; white: hydrogen; red: oxygen).

Schematic drawing to illustrate the Wow in the molecular interaction es.

Boat-to-Boat interconversion/reversion between Boat and Chair induced by heat.

^1H NMR spectra of 2,9-di-CHO, 2,10-di-CHO in $CD_2Cl_2/CS_2 = 4/1$ with the concentration of 2 mg/mL. B and C denote the Boat and Chair conformations, respectively.

Both inter- and intra-molecular hydrogen bonds are present in 1,10-di-Et-amide crystal. Therefore, 1,10-di-Et-amide molecules in polymer form would be oriented so that the two amide groups are connected via intramolecular hydrogen bonds, (position_1 of molecule A) O=C-NH···O=C-NH (position_10 of molecule A). The amide groups of adjacent DBCODs are linked by intermolecular hydrogen bonds, (position_10 of molecule A)

O=C-NH···O=C-NH... (position 1 of molecule B). We will synthesize a series of co-polymers with short and long 1,10-di-Et-amide-containing segments to study the interplay of inter- and intra-molecular forces on the DBCOD conformational preference and activation energy.

CONCLUSION

A low-energy driven shape-changing unit has been highly sought after for years but eluded attainment. Now, for the first time, we demonstrate that two rigid benzene rings fused by a flexible eight-membered cycloalkane with desired substitution property can potentially transform the DBCOD conformational change into a controlled low-energy driven shape-changing event. Experimental investigations, confirmed by theoretical predictions, show that TM-DBCOD requires only 42 kJ/mol to trigger the conformational change from Boat to Chair. Intramolecular hydrogen bonding formed by 1,10-diamide stabilizes Boat over Chair, raising the activation barrier from Boat to Chair up to 68 kJ/mol. This value is much lower than those required by conventional shape-changing molecular structures. Shape-changing will no longer be only reliant on high-energy stimuli.

This work could lay the foundation for scientific exploration of this new low-energy driven shape-changing mechanism that responds to a broad range of low-energy stimulus such as infrared- or magnetically induced heat. Other salient features include (a) innate reversibility arising from the absence of disruption and reformation of covalent bonds during the conformational change, (b) the options of operating in a wide range of solid and liquid media, and (c) high energy throughput as low-energy stimuli are able to penetrate into the entire material.

The creation of low-energy driven shape-changing structures broadens applications especially those that are prone to high-energy damage. This submolecular shape-changing event can potentially act as an actuator in an analog device and as a switch in a logic device. For example, it can be tethered onto biomolecules and incorporated into a polymer chain to achieve stimuli-induced desired functionalities. The geometrical change can also be exploited for pore size modulation of polymer membranes for applications in energy and health. DBCOD embedded polymeric electronic packaging materials could reduce polymer thermal expansion and thus improve reliability of high-density memory devices and possibly realize higher speed logical devices. Furthermore, this work provides insight on how to tailor the energy landscape of medium-sized cyclic structures which frequently act as subunits in natural products.

ASSOCIATED CONTENT

Supporting Information. Detailed information about the synthesis and characterization of DBCOD derivatives, DFT predicted NMR chemical shifts and kinetic and energetic results, rate constants, entropy of activation ($\Delta S^{\ddagger}$) and enthalpy of activation ($\Delta H^{\ddagger}$) for conformational change can be found in Supporting Information. This material is available free of charge via the Internet at http://pubs.acs.org."

AUTHOR INFORMATION

Corresponding Author

*Jennifer Q. Lu, Email: jlu5@ucmerced.edu

Author Contributions

J.Q.L. conceived the project through closely working with W.F. J.Q.L and W.F wrote the manuscript. W.F., J.B. and T.L. performed the synthesis and characterizations of all DBCOD derivatives. W.F. and Y.L. conducted the VT ^{1}H-NMR measurements. J.L., W.T. and T.M.A. performed the DFT calculations to reveal kinetics and thermodynamic energies at different states. T.M.A. performed the predicted ^{1}H-NMR chemical shifts of DBCOD derivatives. R.W.A. evaluated the energy barrier for conformational exchange based on the VT ^{1}H -NMR. S.J.T. conducted the X-ray single-crystal diffraction measurements. W.F., R.W.A., S.J.T., B.J.S., T.M.A., W.Y., Y.L. and J.Q.L discussed the data processing, analysis and interpretation.

Notes

The authors declare no competing interests.

ACKNOWLEDGMENT

REFERENCES

(1) Kamiya, Y.; Asanuma, H. Light-Driven DNA Nanomachine with a Photoresponsive Molecular Engine. *Accounts Chem. Res.* **2014**, *47*, 1663-1672.

(2) Li, X.; Zhai, T.; Gao, P.; Cheng, H.; Hou, R.; Lou, X.; Xia, F. Role of Outer Surface Probes for Regulating Ion Gating of Nanochannels. *Nat. Commun.* **2018**, *9*, 40.

(3) Mura, S.; Nicolas, J.; Couvreur, P. Stimuli-responsive Nanocarriers for Drug Delivery. *Nat. Mater.* **2013**, *12*, 991-1003.

(4) Zeng, Y.; Lu, J. Q. Optothermally Responsive Nanocomposite Generating Mechanical Forces for Cells Enabled by Few-Walled Carbon Nanotubes. *ACS Nano* **2014**, *8*, 11695-11706.

(5) Lancia, F.; Ryabchun, A.; Nguindjel, A.-D.; Kwangmettatam, S.; Katsonis, N. Mechanical Adaptability of Artificial Muscles from Nanoscale Molecular Action. *Nat. Commun.* **2019**, *10*, 4819.

(6) Li, C. S.; Liu, Y.; Huang, X. Z.; Jiang, H. R. Direct Sun-Driven Artificial Heliotropism for Solar Energy Harvesting Based on a Photo-Thermomechanical Liquid-Crystal Elastomer Nanocomposite. *Adv. Funct. Mater.* **2012**, *22*, 5166-5174.

(7) Aßhoff, S. J.; Lancia, F.; Iamsaard, S.; Matt, B.; Kudernac, T.; Fletcher, S. P.; Katsonis, N. High-Power Actuation from Molecular Photoswitches in Enantiomerically Paired Soft Springs. *Angew. Chem. Int. Edit.* **2017**, *56*, 3261-3265.

(8) White, T. J.; Broer, D. J. Programmable and Adaptive Mechanics with Liquid Crystal Polymer Networks and Elastomers. *Nat. Mater.* **2015**, *14*, 1087-1098.

(9) Cadogan, D.; Scarborough, S., Rigidizable Materials for Use in Gossamer Space Inflatable Structures. In *19th AIAA Applied Aerodynamics Conference*.

(10) Rossiter, J.; Takashima, K.; Scarpa, F.; Walters, P.; Mukai, T. Shape Memory Polymer Hexachiral Auxetic Structures with Tunable Stiffness. *Smart Mater. Struct.* **2014**, *23*, 045007.

(11) Takashima, K.; Sugitani, K.; Morimoto, N.; Sakaguchi, S.; Noritsugu, T.; Mukai, T. Pneumatic Artificial Rubber Muscle Using Shape-Memory Polymer Sheet With Embedded Electrical Heating Wire. *Smart Mater. Struct.* **2014**, *23*.

(12) Hou, L.; Zhang, X.; Cotella, G. F.; Carnicella, G.; Herder, M.; Schmidt, B. M.; Pätzel, M.; Hecht, S.; Cacialli, F.; Samorì, P. Optically Switchable Organic Light-Emitting Transistors. *Nat. Nanotechnol.* **2019**, *14*, 347-353.

(13) Leydecker, T.; Herder, M.; Pavlica, E.; Bratina, G.; Hecht, S.; Orgiu, E.; Samorì, P. Flexible Non-Volatile Optical Memory Thin-Film Transistor Device with over 256 Distinct Levels Based on An Organic Bicomponent Blend. *Nat. Nanotechnol.* **2016**, *11*, 769-775.

(14) Schmittel, M.; De, S.; Pramanik, S. Reversible ON/OFF Nanoswitch for Organocatalysis: Mimicking the Locking and Unlocking Operation of CaMKII. *Angew. Chem. Int. Edit.* **2012**, *51*, 3832-3836.

(15) Landge, S. M.; Aprahamian, I. A pH Activated Configurational Rotary Switch: Controlling the E/Z Isomerization in Hydrazones. *J. Am. Chem. Soc.* **2009**, *131*, 18269-18271.

(16) Harris, J. D.; Moran, M. J.; Aprahamian, I. New Molecular Switch Architectures. *Proc. Natl. Acad. Sci. U. S. A.* **2018**, *115*, 9414-9422.

(17) Collins, B. S. L.; Kistemaker, J. C. M.; Otten, E.; Feringa, B. L. A Chemically Powered Unidirectional Rotary Molecular Motor Based on A Palladium Redox Cycle. *Nat. Chem.* **2016**, *8*, 860-866.

(18) Yin, X.; Zang, Y.; Zhu, L.; Low, J. Z.; Liu, Z.-F.; Cui, J.; Neaton, J. B.; Venkataraman, L.; Campos, L. M. A Reversible Single-Molecule Switch Based on Activated Antiaromaticity. *Sci Adv* **2017**, *3*, eaao2615.

(19) Liu, Y.; Flood, A. H.; Stoddart, J. F. Thermally and Electrochemically Controllable Self-Complexing Molecular Switches. *J. Am. Chem. Soc.* **2004**, *126*, 9150-9151.

(20) Bandara, H. M. D.; Burdette, S. C. Photoisomerization in Different Classes of Azobenzene. *Chem. Soc. Rev.* **2012**, *41*, 1809-1825.

(21) Feringa, B. L.; van Delden, R. A.; Koumura, N.; Geertsema, E. M. Chiroptical Molecular Switches. *Chem. Rev.* **2000**, *100*, 1789-1816.

(22) Guo, X.; Zhou, J.; Siegler, M. A.; Bragg, A. E.; Katz, H. E. Visible-Light-Triggered Molecular Photoswitch Based on Reversible E/Z Isomerization of a 1,2-Dicyanoethene Derivative. *Angew. Chem. Int. Edit.* **2015**, *54*, 4782-4786.

(23) Ryabchun, A.; Li, Q.; Lancia, F.; Aprahamian, I.; Katsonis, N. Shape-Persistent Actuators from Hydrazone Photoswitches. *J. Am. Chem. Soc.* **2019**, *141*, 1196-1200.

(24) Irie, M. Diarylethenes for Memories and Switches. *Chem. Rev.* **2000**, *100*, 1685-1716.

(25) Irie, M.; Fukaminato, T.; Matsuda, K.; Kobatake, S. Photochromism of Diarylethene Molecules and Crystals: Memories, Switches, and Actuators. *Chem. Rev.* **2014**, *114*, 12174-12277.

(26) Klajn, R. Spiropyran-based Dynamic Materials. *Chem. Soc. Rev.* **2014**, *43*, 148-184.

(27) de Villeneuve, C. H.; Michalik, F.; Chazalviel, J. N.; Rück-Braun, K.; Allongue, P. Quantitative IR Readout of Fulgimide Monolayer Switching on Si(111) Surfaces. *Adv. Mater.* **2013**, *25*, 416-421.

(28) Yokoyama, Y. Fulgides for Memories and Switches. *Chem. Rev.* **2000**, *100*, 1717-1740.

(29) Goulet-Hanssens, A.; Eisenreich, F.; Hecht, S. Enlightening Materials with Photoswitches. *Adv. Mater.* **2020**, *32*, 1905966.

(30) Pianowski, Z. L. Recent Implementations of Molecular Photoswitches into Smart Materials and Biological Systems. *Chem.-Eur. J.* **2019**, *25*, 5128-5144.

(31) Dong, M.; Babalhavaeji, A.; Collins, C. V.; Jarrah, K.; Sadovski, O.; Dai, Q.; Woolley, G. A. Near-Infrared Photoswitching of Azobenzenes under Physiological Conditions. *J. Am. Chem. Soc.* **2017**, *139*, 13483-13486.

(32) Hammerich, M.; Schütt, C.; Stähler, C.; Lentes, P.; Röhricht, F.; Höppner, R.; Herges, R. Heterodiazocines: Synthesis and Photochromic Properties, Trans to Cis Switching within the Bio-optical Window. *J. Am. Chem. Soc.* **2016**, *138*, 13111-13114.

(33) Zulfikri, H.; Koenis, M. A. J.; Lerch, M. M.; Di Donato, M.; Szymanski, W.; Filippi, C.; Feringa, B. L.; Buma, W. J. Taming the Complexity of Donor-Acceptor Stenhouse Adducts: Infrared Motion Pictures of the Complete Switching Pathway. *J. Am. Chem. Soc.* **2019**, *141*, 7376-7384.

(34) Lerch, M. M.; Szymanski, W.; Feringa, B. The (Photo)Chemistry Of Stenhouse Photoswitches: Guiding Principles And System Design. *Chem. Soc. Rev.* **2018**, *47*, 1910-1937.

(35) Yoshino, T.; Kondo, M.; Mamiya, J.-i.; Kinoshita, M.; Yu, Y.; Ikeda, T. Three-Dimensional Photomobility of Crosslinked Azobenzene Liquid-Crystalline Polymer Fibers. *Adv. Mater.* **2010**, *22*, 1361-1363.

(36) Perutz, M. F. Mechanisms Regulating the Reactions of Human Hemoglobin With Oxygen and Carbon Monoxide. *Annu. Rev. Physiol.* **1990**, *52*, 1-26.

(37) Li, J.; Ning, Y.; Hedley, W.; Saunders, B.; Chen, Y.; Tindill, N.; Hannay, T.; Subramaniam, S. The Molecule Pages database. *Nature* **2002**, *420*, 716-717.

(38) Ugur, G.; Chang, J.; Xiang, S.; Lin, L.; Lu, J. A Near-Infrared Mechano Responsive Polymer System. *Adv. Mater.* **2012**, *24*, 2685-2690.

(39) Shen, X.; Viney, C.; Johnson, E. R.; Wang, C.; Lu, J. Q. Large Negative Thermal Expansion of A Polymer Driven by A Submolecular Conformational Change. *Nat. Chem.* **2013**, *5*, 1035-1041.

(40) Shen, X.; Connolly, T.; Huang, Y.; Colvin, M.; Wang, C.; Lu, J. Adjusting Local Molecular Environment for Giant Ambient Thermal Contraction. *Macromol. Rapid Commun.* **2016**, *37*, 1904-1911.

(41) Weston, C. E.; Richardson, R. D.; Haycock, P. R.; White, A. J. P.; Fuchter, M. J. Arylazopyrazoles: Azoheteroarene Photoswitches Offering Quantitative Isomerization and Long Thermal Half-Lives. *J. Am. Chem. Soc.* **2014**, *136*, 11878-11881.

(42) Crecca, C. R.; Roitberg, A. E. Theoretical Study of the Isomerization Mechanism of Azobenzene and Disubstituted Azobenzene Derivatives. *J. Phys. Chem. A* **2006**, *110*, 8188-8203.

(43) Crossley, R.; Downing, A. P.; Nogradi, M.; Bragadeo.A; Ollis, W. D.; Sutherla.Io Conformational Behavior of Medium-Sized Rings. Part 1. 5,6,11,12-Tetrahydrodibenzo[a,e]cyclo-octene (1,2,5,6-Dibenzocyclo-Octa-1,5-Diene) and Heterocyclic Analogs. *J. Chem. Soc.-Perkin Trans. 1* **1973**, 205-217.

(44) Allisy-Roberts, P.; Williams, J., Chapter 1 - Radiation physics. In *Farr's Physics for Medical Imaging (Second Edition)*, Allisy-Roberts, P.; Williams, J., Eds. W.B. Saunders: 2008; pp 1-21.

(45) Hu, H.; Boone, A.; Yang, W. Mechanism of OMP Decarboxylation in Orotidine 5′-Monophosphate Decarboxylase. *J. Am. Chem. Soc.* **2008**, *130*, 14493-14503.

(46) Kuhn, B.; Kollman, P. A. QM−FE and Molecular Dynamics Calculations on Catechol O-Methyltransferase: Free Energy of Activation in the Enzyme and in Aqueous Solution and Regioselectivity of the Enzyme-Catalyzed Reaction. *J. Am. Chem. Soc.* **2000**, *122*, 2586-2596.

(47) Massey, V.; Curti, B.; Ganther, H. A Temperature-Dependent Conformational Change in D-Amino Acid Oxidase and Its Effect on Catalysis. *J. Biol. Chem.* **1966**, *241*, 2347-2357.

(48) Wang, Z.; Huang, Y. H.; Guo, J.; Li, Z. H.; Xu, J. T.; Lu, J. Q.; Wang, C. C. Design and Synthesis of Thermal Contracting Polymer with Unique Eight-Membered Carbocycle Unit. *Macromolecules* **2018**, *51*, 1377-1385.

(49) Levick, M. T.; Coote, S. C.; Grace, I.; Lambert, C.; Turner, M. L.; Procter, D. J. Phase Tag-Assisted Synthesis of Benzo[b]carbazole End-Capped Oligothiophenes. *Org. Lett.* **2012**, *14*, 5744-5747.

(50) Baker, W.; Banks, R.; Lyon, D. R.; Mann, F. G. 10. The Action of Sodium on o-Xylylene Dibromide. *J. Chem. Soc.* **1945**, 27-30.

(51) Hamza, A. Gas-Phase Conformations and Exciton Couplings in 5,6,11,12-Tetrahydrodibenzo[A,E]cyclooctene. *Struct. Chem.* **2010**, *21*, 787-793.

(52) Sekine, Y.; Boekelheide, V. A Study of The Synthesis and Properties of [26](1,2,3,4,5,6)cyclophane (superphane). *J. Am. Chem. Soc.* **1981**, *103*, 1777-1785.

(53) Sekine, Y.; Brown, M.; Boekelheide, V. [2.2.2.2.2.2] (1,2,3,4,5,6)Cyclophane: Superphane. *J. Am. Chem. Soc.* **1979**, *101*, 3126-3127.

(54) Wang, Z.; Huang, Y.; Guo, J.; Li, Z.; Xu, J.; Lu, J. Q.; Wang, C. Design and Synthesis of Thermal Contracting Polymer with Unique Eight-Membered Carbocycle Unit. *Macromolecules* **2018**, *51*, 1377-1385.

(55) Dalcanale, E.; Montanari, F. Selective Oxidation of Aldehydes to Carboxylic Acids with Sodium Chlorite-Hydrogen Peroxide. *J. Org. Chem.* **1986**, *51*, 567-569.

(56) Witosińska, A.; Musielak, B.; Serda, P.; Owińska, M.; Rys, B. Conformation of Eight-Membered Benzoannulated Lactams by Combined NMR and DFT Studies. *J. Org. Chem.* **2012**, *77*, 9784-9794.

(57) Mitchell, R. H. Conformational Changes of 2,11-Dithia[3.3]metacyclophane. A New Look Using VT NMR

and Calculation. *J. Am. Chem. Soc.* **2002**, *124*, 2352-2357.

(58) Sauriol-Lord, F.; St-Jacques, M. Stereodynamic Investigation of Dibenzo-1,5-cyclooctadiene and 5,6,11,12-tetrahydrodibenzo[b,f] [1,4]diazocine Derivatives. *Can. J. Chem.* **1975**, *53*, 3768-3776.

(59) Montecalvo, D.; St. Jacques, M.; Wasylishen, R. Direct Observation of Chair and Boat Conformations for Dibenzocycloocta-1,5-Diene by Nuclear Magnetic Resonance. *J. Am. Chem. Soc.* **1973**, *95*, 2023-2024.

(60) Nishimura, N.; Sueyoshi, T.; Yamanaka, H.; Imai, E.; Yamamoto, S.; Hasegawa, S. Thermal Cis-to-Trans Isomerization of Substituted Azobenzenes .2. Substituent and Solvent Effects. *Bull. Chem. Soc. Jpn.* **1976**, *49*, 1381-1387.

(61) Joshi, N. K.; Fuyuki, M.; Wada, A. Polarity Controlled Reaction Path and Kinetics of Thermal Cis-to-Trans Isomerization of 4-Aminoazobenzene. *J. Phys. Chem. B* **2014**, *118*, 1891-1899.

(62) Brown, E. V.; Granneman, G. R. Cis-Trans Isomerism in The Pyridyl Analogs of Azobenzene. Kinetic and Molecular Orbital Analysis. *J. Am. Chem. Soc.* **1975**, *97*, 621-627.

(63) Dokić, J.; Gothe, M.; Wirth, J.; Peters, M. V.; Schwarz, J.; Hecht, S.; Saalfrank, P. Quantum Chemical Investigation of Thermal Cis-to-Trans Isomerization of Azobenzene Derivatives: Substituent Effects, Solvent Effects, and Comparison to Experimental Data. *J. Phys. Chem. A* **2009**, *113*, 6763-6773.

(64) Norio, N.; Shinya, K.; Yoshimi, S. The Thermal Isomerization of Azobenzenes. III. Substituent, Solvent, and Pressure Effects on the Thermal Isomerization of Push-pull Azobenzenes. *Bull. Chem. Soc. Jpn.* **1984**, *57*, 1617-1625.

(65) Liu, L.; Guo, Q.-X. Isokinetic Relationship, Isoequilibrium Relationship, and Enthalpy−Entropy Compensation. *Chem. Rev.* **2001**, *101*, 673-696.

(66) Domiano, P.; Cozzini, P.; Claramunt, R. M.; Lavandera, J. L.; Sanz, D.; Elguero, J. The Molecular Structure of 6, 8, 6 and Related Systems. *J. Chem. Soc.-Perkin Trans. 2* **1992**, 1609-1620.

For Table of Contents Only: